Materials for Renewable and Sustainable Energy
https://doi.org/10.1007/s40243-024-00259-6

ORIGINAL PAPER

Maximizing power generation in single-chamber microbial fuel cells: the role of $LiTa_{0.5}Nb_{0.5}O_3$/g-C_3N_4 photocatalyst

Nour-eddine Lazar[1] · Driss Mazkad[1] · Hamza Kharti[5] · Fatma Yalcinkaya[2] · Andrea Pietrelli[3] · Vincenzo Ferrara[4] · Noureddine Touach[1] · Abdellah Benzaouak[1] · Mohammed El Mahi[1] · El Mostapha Lotfi[1]

Received: 22 November 2023 / Accepted: 18 March 2024

Abstract

Microbial fuel cells (MFCs) have attracted a great deal of attention as a promising technology for recovering electricity from organic substances by harnessing the metabolic activities of microorganisms. The objective of this study is to assess the efficacy of a $LiTa_{0.5}Nb_{0.5}O_3$/g-C_3N_4 (LTN/g-C_3N_4) heterojunction as a photocathode catalyst within a single-chamber microbial fuel cell operating under both light irradiation and dark conditions. X-Ray diffraction (XRD), Fourier transform infrared spectroscopy (FTIR), scanning electron microscopy (SEM), and Energy dispersive X-Ray spectroscopy (EDS) were used to conduct a comprehensive analysis of the composite catalyst, revealing its exceptional purity and unique properties. After 120 h of exposure to visible light, the maximal power density of the MFC containing LTN/g-C3N4-modified carbon cloth was determined to be 667.7 mW/m^3. The power density achieved with the presence of light was approximately three times greater than the power density obtained without light in the MFC (235.64 mW/m^3). In addition, the study determined that the removal efficiencies of chemical oxygen demand (COD) were 88.4% and 66.5% when exposed to light and in the absence of light, respectively. These findings highlight the potential of the non-precious LTN/g-C_3N_4 photocatalyst as a viable alternative for effective wastewater treatment and power generation in microbial fuel cells with a single chamber configuration.

Keywords Single-chamber MFC · LTN/g-C_3N_4 heterojunction · Cathode photocatalyst · Bioelectricity

Introduction

Meeting increased demand for energy production is proving difficult for the power industry. In addition, one-fourth of the global population lacks access to pure water and sanitation, which is a major global concern [1]. Therefore, the extracting of organic compounds or energy from wastewater has the potential to significantly decrease the expenses associated with wastewater treatment and contribute to the preservation of energy resources [2, 3].

Numerous initiatives have been undertaken to develop novel methods for generating renewable energy. The microbial fuel cell (MFC) is a method that has garnered significant interest as a potentially viable technology capable of concurrently producing electricity and treating wastewater [4].

MFCs are a type of microbial electrochemical technology (MET) that employ biocatalytic reactions at the bioanode to generate electrical energy from organic wastewater [5–9]. In the MFC, the anode compartment contains electrogenic

✉ Nour-eddine Lazar
noureddinelazar@yahoo.fr

1 Laboratory of Spectroscopy, Molecular Modeling, Materials, Nanomaterials, Water and Environment, Materials for Environment Team, ENSAM, Mohammed V University, Rabat, Morocco

2 Faculty of Mechatronics, Informatics and Interdisciplinary Studies, Technical University of Liberec, Liberec, Czech Republic

3 Univ Lyon, Université Claude Bernard Lyon 1, INSA LYON, Ecole Centrale Lyon, CNRS, UMR 5005 Ampere, Villeurbanne F69622, France

4 Department of Information Engineering, Electronics and Telecommunications, University of Rome La Sapienza, Via Eudossiana 18, Rome 00184, Italy

5 Geo-Biodiversity and Natural Patrimony Laboratory (GEOBIO), Scientific Institute Mohammed V University in Rabat, Avenue Ibn Batouta, P.B. 703, Rabat-Agdal 10106, Morocco

Published online: 09 May 2024

microorganisms that oxidize organic matter to release electrons. These electrons are then collected by the anode and transferred to the cathode, where they interact with protons, resulting in the reduction of electron acceptors and generation of power that can be harnessed through a circuit [10]. The efficiency of an MFC can be influenced by various factors, such as the type of bacteria, the choice of electrode materials, the chemical substrate, the pH and temperature conditions, the membrane employed, as well as the internal and external resistance of the cell [11]. However, it is important to note that the cathode, which plays a vital role in determining the overall efficiency of the MFC system, has significant impact on both performance and cost [12].

Based on the conducted research, it has been observed that the utilization of metallic electrodes in MFC yields significant advantages in terms of generating increased levels of current and voltage. Furthermore, single-chamber MFCs have been found to achieve greater current and power density values [13]. However, the efficiency of the process is dependent on the specific catalyst employed.

Microbes on a carbon electrode serve as the catalyst at the anode in an MFC. Consequently, it is essential to identify an appropriate catalyst for the cathode. Noble metal-based materials, including palladium (Pd) and platinum (Pt), have been widely utilized as cathodic catalysts in order to improve the kinetics of the oxygen reduction reaction (ORR) occurring on the surface of the cathode [11].Regrettably, the utilization of these catalysts in practical applications is restricted due to their exorbitant cost [14–16]. Researchers from diverse fields have united to improve materials for enhancing the oxygen reduction reaction (ORR) in neutral media. Among these, M-N-C catalysts (where M represents a transition metal) offer a promising alternative to traditional materials like Pt, Pd, or activated carbon (AC). These catalysts demonstrate superior performance and remarkable durability over extended operational periods. Consequently, they emerge as prime candidates for optimization efforts aimed at boosting microbial fuel cell (MFC) power output [17]. Various carbon materials, such as carbon cloth, carbon fiber brush, carbon felt, carbon nanofiber, carbon paper, graphite poles, and graphite plates, have typically been investigated as potential replacements for Pt-based cathode catalysts for 4-electron ORR. The motivation behind exploring these carbon materials lies in their cost-effectiveness and superior catalytic activity compared to Pt-based catalysts. Nonetheless, it is important to note that carbon-based materials typically demonstrate a comparatively diminished microbial inoculum and electron transfer efficiency. To tackle this issue, one of the promising solutions is to modify the carbon-based anodes to enhance microbial immobilization, reduce electron transfer barriers, and ultimately promote MFC electricity generation. Therefore, it is worthwhile to develop novel catalysts to enhance cathodic performance [18, 19].

Previous studies have indicated that Perovskite-type oxides derived from lithium niobite ($LiNbO_3$) and lithium tantalite ($LiTaO_3$) are commonly employed as photocatalysts in single-chambered MFCs. It has been demonstrated that the application of light to these materials results in a power density of 131 mW/m^3, a value that is three times greater than the power generated by $LiNbO_3$ in the absence of light [11]. Similarly, the power density and open-circuit voltage (OCV) of $LiTaO_3$ [20] were observed to experience an increase from 17 to 55 mW/m3 and 158 to 349 mV, respectively, when exposed to light. The performance of $Li_{0.95}Ta_{0.57}Nb_{0.38}Cu_{0.15}O_3$ was further examined by Louki et al. [21], who employed both slow and rapid cooling techniques during the preparation process. They found that the maximum power densities were 20.10 and 205.35 mW/m^3, respectively.

Crafting the cathode of microbial electrolysis cells (MECs) using light-responsive photocatalytic materials is an effective strategy for increasing the circuital current and improving the rates of chemical and heavy metal reduction. These light-active materials generate photogenerated conduction band electrons when exposed to artificial or solar light, which can facilitate the reduction of electrotrophs and heavy metal ions. Moreover, the utilization of these materials has the potential to decrease the interfacial resistance at the cathode, resulting in an enhancement of the external circuital current of the cell [22]. In order to accomplish this objective, the utilization of graphitic carbon nitride ($g\text{-}C_3N_4$) has been proposed as a viable semiconductor photocatalyst due to its efficient reduction capabilities, economical nature, exceptional stability, and responsiveness to visible light. The material exhibits a band gap of approximately 2.7 eV and a conduction band edge position of 1.2 eV relative to the standard hydrogen electrode (SHE), indicating its significant efficacy in facilitating reduction reactions [23].

The aim of this study is to evaluate the potential application of $g\text{-}C_3N_4/LiNb_{0.5}Ta_{0.5}O_3$ as a cathodic photo-electrocatalyst within a single-chamber MFC setup, under conditions with and without exposure to visible light. The goal of this study is to examine the photo-electrocatalytic behavior of the material in order to ascertain its potential for enhancing power generation. This suggests the first example in which this particular combination of materials has been employed within MFC system.

Experimental

Photocatalyst synthesis

Preparation of $LiTa_{0.5}Nb_{0.5}O_3$

The synthesis of $LiTa_{0.5}Nb_{0.5}O_3$ (LTN) was carried out using high-purity precursors include Li_2CO_3 (98%, Panreac), Ta_2O_5 (99%, Aldrich), and Nb_2O_5 (99.5%, Aldrich) via the conventional solid-state method. The oxides underwent ball milling using agate balls and an adequate amount of alcohol. Afterwards, they were transferred into an alumina boat for calcination at various temperatures. The calcination process was initiated at a temperature of 600 ºC in order to facilitate the release of CO_2. Subsequently, the temperature was gradually raised to 800 ºC, 1000 ºC, and 1100 ºC respectively. This process was carried out for a duration of 12 h within a muffle furnace.

Preparation of g-C_3N_4

The preparation of g-C_3N_4 sheets involved annealing urea in a semi-closed system with modifications to the method described by Zhang et al. [24] Specifically, 10 g of urea was placed into a crucible and heated to 550 °C for 4 h in a furnace with a heating rate of 5 °C/min. The resulting yellow product was collected after cooling down to room temperature naturally and ground into a powder using an agate mortar, and was subsequently referred to as g-C_3N_4.

Preparation of LTN / g-C_3N_4 heterojunction

The binary mixture of 15% LTN and 85% / g-C_3N_4, based on weight ratio, was synthesized using a straightforward solid-state method. A typical experimental procedure was as follows: 0.15 g of LTN and 0.85 g of g-C_3N_4 were subjected to ball milling using agate balls for a duration of 30 min. Subsequently, the resultant mixture was transferred to a crucible and underwent calcination at a temperature of 550 °C for a duration of 2 h. The resultant outcome of this procedure yielded a yellow substance, which was identified and labeled as LTN/g-C_3N_4.

Preparation of LTN / g-C_3N_4 coated cathode

In order to prepare the working electrode, a solution containing the catalyst powder (60 mg/cm^2) deionized water, isopropanol, and polytetrafluoroethylene (PTFE) (solid, Sigma-Aldrich, Burlington, MA, USA) was created with a mass ratio of 1:9 (solution : catalyst) [25], The resulting mixture was then applied onto a carbon cloth with a surface area of 1 cm^2 using mechanical pressure. Subsequently, the coated carbon cloth was left to dry overnight under ambient conditions, resulting in the formation of a thin film.

Photocatalyst characterization

The X-ray diffraction (XRD) technique was employed to examine the crystal structure of g-C_3N_4, LTN, and LTN/g-C_3N_4 photocathodes. The analysis was conducted using a PANalytical X'Pert PRO diffractometer, with Cu-Kα radiation (λ = 1.549 Å), over a 2θ range spanning from 10° to 80°. The QUATTRO S-FEG-Thermofisher scanning electron microscope was utilized to examine the surface morphology of the synthesized particles. In order to analyze the functional groups present in the materials, an Fourier-transform infrared spectroscopy (FTIR) (PerkinElmer Spectrum two) was used. In addition, a Perkin Elmer Lambda 900 UV/Vis spectrometer with an integrating sphere was used to generate the UV-Vis diffuse reflectance spectrum (UV-Vis DRS), allowing analysis of the band gap and optical properties of the materials.

Wastewater

The analysis of the industrial wastewater sample revealed a chemical oxygen demand (COD) concentration of 1740 mg/L and a pH value of 7.3. In order to preserve the integrity of the wastewater, the gathered sample was stored within a cold environment. The chemical oxygen demand (COD) was measured in accordance with the American Public Health Association's (APHA) established protocol [26], using a photoLab 7600 UV-visible spectrophotometer manufactured by WTW, Germany.

MFC configuration and operation

A cylindrical glass bottle with flanges (Schott Duran, Germany) was utilized to construct a Microbial Fuel Cell (MFC) with a single chamber. The total volume of the MFC was 250 mL. The composition of the anode consisted of 100 cm3 of graphite granules and a graphite rod with a diameter of 3 mm. This graphite rod was connected to the cathode electrode via an external resistance of 1 kΩ. In order to enhance the division between the anode and cathode, a proton exchange membrane, specifically Nafion (NRE-212), was used. The membrane underwent a series of treatments in order to condition it before implementation. Initially, the sample was immersed for one hour in a 3% hydrogen peroxide solution at 80 °C and a concentration of 3 mM. Subsequently, it was submerged in a sulfuric acid solution with a molarity of 0.5 M for an additional hour.

The anodic chamber was filled with 160 mL of feed and tightly sealed with lids in order to create and maintain

anaerobic conditions. To maintain a constant operating temperature throughout the duration of the experiment, a jacket and a thermostatic bath manufactured by Selecta in Spain were utilized. Figure 1 shows a schematic representation of the experimental apparatus. A total duration of five days was designated for the testing process, during which the Metal-Organic Framework Composite (MFC) was subjected to illumination by visible light utilizing a 20-Watt Light Emitting Diode (LED) light source.

Measurement and analysis of single-chamber MFC operation

To perform a comprehensive examination of the Microbial Fuel Cell (MFC) performance, the operating voltage was carefully monitored at regular hourly intervals using a precise variable resistor box. In order to ensure precise measurements during the subsequent polarization study, the MFC was initially operated in open circuit mode. This provided an ample duration for the MFC to achieve its maximum open circuit voltage (OCV), a crucial parameter for subsequent analysis.

To characterize the power density and polarization behavior of the MFC, the voltage (V) and current (I) were systematically measured across a diverse range of external loads. These loads encompassed a spectrum of resistance values, spanning from 11 MΩ down to 1Ω. The construction of voltage-current (V-I) curves required a stepwise variation of the resistor from high to low resistance values. The voltage and current were recorded once they reached a steady-state, ensuring reliable and consistent data acquisition.

The internal resistance of the MFC was subsequently determined by calculating the slope of the I-V curve on the polarization graph. This parameter provides valuable insights into the overall performance and efficiency of the MFC system [27].

Equations (1) and (2) were employed to evaluate the power density (P) and current density (I), respectively.

$$P = V \times I/A \tag{1}$$

$$I = V_{(cellvoltage)}/R_{ext} \tag{2}$$

Here, I represents the current, V denotes the voltage, R signifies the resistance, and A represents the area of the electrode. These equations offer a quantitative understanding of the power and current characteristics of the MFC system.

In addition, an evaluation was conducted to assess the COD of the wastewater inlet and effluent within the anode chamber, with the aim of determining the efficacy of the MFC in removing COD. The COD determination was carried out using a spectrophotometric method with a Spectroquant Nova 30 spectrophotometer manufactured by Merck. The percentage COD removal was calculated using the Eq. 3:

$$CODremoval\% = \frac{[\mathrm{COD}]\,\mathrm{i} - [\mathrm{COD}]\,\mathrm{f}}{[\mathrm{COD}]\,\mathrm{i}} \times 100. \tag{3}$$

where [COD]i (mg/L) refers to the initial COD charge in the wastewater entering the anode chamber and [COD]f (mg/L) reflects the final COD concentration of the effluent in the anode chamber following the experiment.

Results and discussion

Characterization

Figure 2 depicts the X-ray diffraction (XRD) patterns of g-C3N4, LTN, and LTN/g-C3N4 heterojunction samples. The X-ray diffraction (XRD) analysis demonstrates that the diffraction pattern of the LTN phase closely corresponds

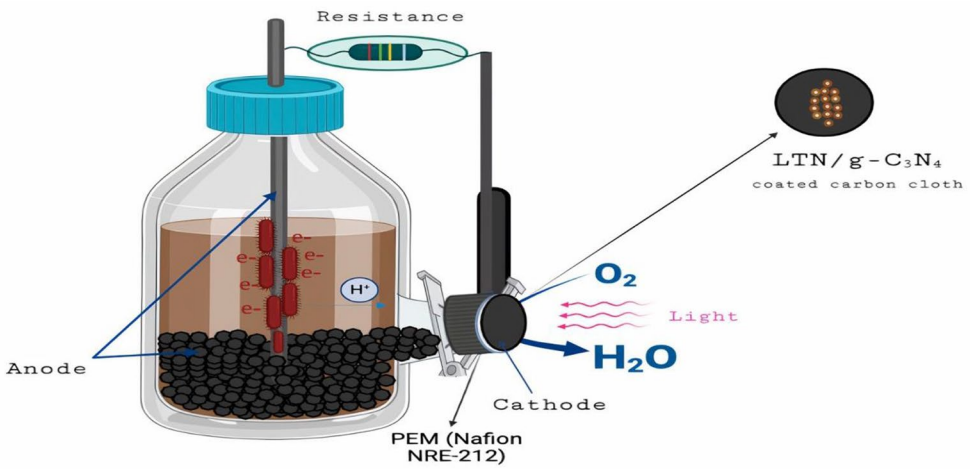

Fig. 1 Schematic representation of the single-chamber MFC

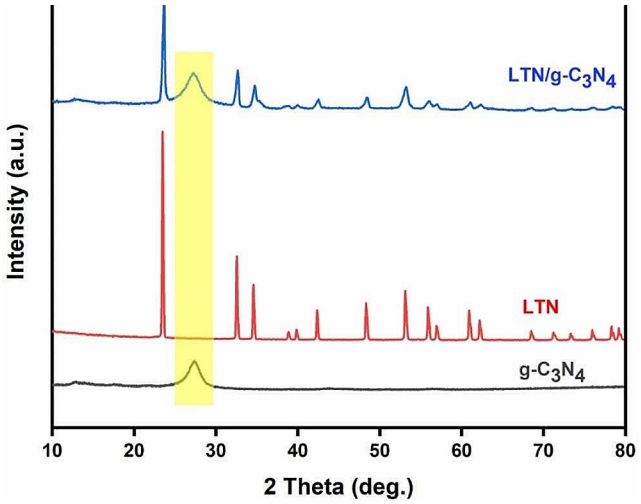

Fig. 2 XRD pattern of g-C_3N_4, LTN and LTN/g-C_3N_4 heterojunction material

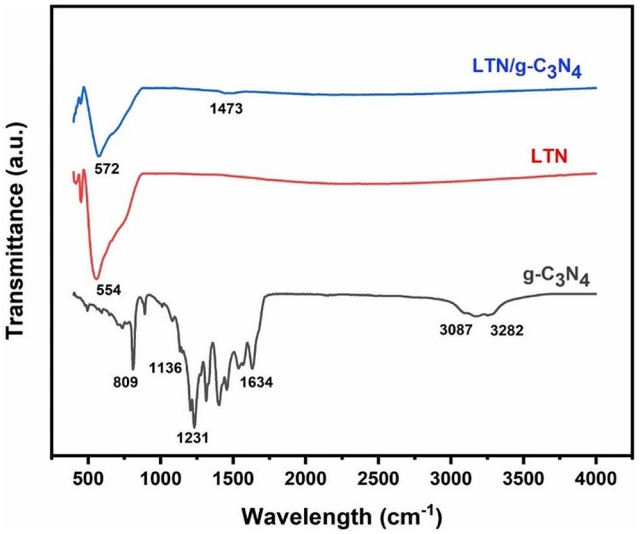

Fig. 3 FTIR spectrum of g-C_3N_4, LTN and LTN/g-C_3N_4 heterojunction material

to the standard lithium niobite (JCPDS No. 020–0631), suggesting a trigonal symmetry characterized by a space group of R3c. The peak observed at an angle of 27.36° in the pure g-C_3N_4 sample corresponds to the distinctive interplanar stacked graphitic layered structure and specifically represents the (002) plane, as identified by the JCPDS file No. 87-1526. These peaks are aligned with the findings of g-C_3N_4 and LTN as documented in prior research papers [28, 29]. Nevertheless, it is worth noting that in the LTN/ g-C_3N_4 heterojunction, the diffraction patterns belong to LTN and g-C_3N_4, exclusively correspond to LTN and g-C3N4, without any discernible diffraction peaks originating from additional impurities. This discovery validates that both LTN and g-C_3N_4 retain their inherent crystal structure without undergoing any formation of additional impurities throughout the synthesis procedure. The confirmation of the presence of the LTN/g-C_3N_4 heterojunction photocathode is subsequently discussed through the utilization of Furrier-transform infrared spectroscopy (FTIR), as elaborated upon in subsequent sections.

The FTIR analysis was conducted to examine the structural features and functional groups present in the materials g-C_3N_4, LTN, and heterojunction material LTN/ g-C_3N_4. Figure 3 illustrates the peaks obtained from the analysis. The spectrum of pure g-C_3N_4 spectrum exhibits a peak at 809 cm^{-1}, which can be attributed to the breath mode of the s-triazine unit [30, 31]. Furthermore, an intense peak ranging from 1136 to 1634 cm^{-1} was detected, indicating the presence of a robust bond. This peak aligns with the anticipated stretching vibration of conjugated CN heterocycles, signifying the characteristic features of carbon nitride [28, 31]. Moreover, a wide spectral range spanning from 3087 to 3282 cm^{-1} was attributed to the stretching vibrations of N-H and O-H bonds that are inherent in the photocatalysts [32].

In contrast, both LTN and LTN/ g-C_3N_4 exhibited a comparable spectral pattern within the 554–572 cm^{-1} range, which can be attributed to the vibration of Nb\O [33] and Ta\O [34]. Furthermore, a small band at 1473 cm^{-1} was observed in the LTN/g-C3N4 spectrum, originating from the aromatic C–N stretching. This finding suggests the formation of a heterojunction structure between the two materials, indicating their binding nature.

The surface morphological characteristics of the as-synthesized LTN/ g-C_3N_4 hybrid material were thoroughly examined utilizing Scanning Electron Microscopy (SEM) techniques. The obtained results, as depicted in Fig. 4(a), confirmed the successful synthesis of nanosheets-like stacked g-C_3N_4, which served as the host structure for the intricate loading of LTN particles. The micrograph exhibited a high level of resolution, revealing a distinct organization of g-C_3N_4 nanosheets. This arrangement formed a hierarchical structure that enhanced the dispersion and immobilization of LTN particles. On the other hand,, Fig. 4(b) presents an illustration of the LTN particles, showcasing their characteristic spherical morphology. The particles were observed to exhibit a tendency for aggregation, resulting in the formation of significantly large masses with an estimated size of approximately 1.89 µm. This phenomenon serves to emphasize the interaction between the LTN particles and the g-C_3N_4 nanosheets. The present studies have contributed to a deeper comprehension of the structural attributes and arrangement of the LTN/g-C_3N_4 heterojunction. Furthermore, these investigations have yielded valuable insights into the potential applications of this heterojunction across diverse domains of scientific inquiry and technological advancements.

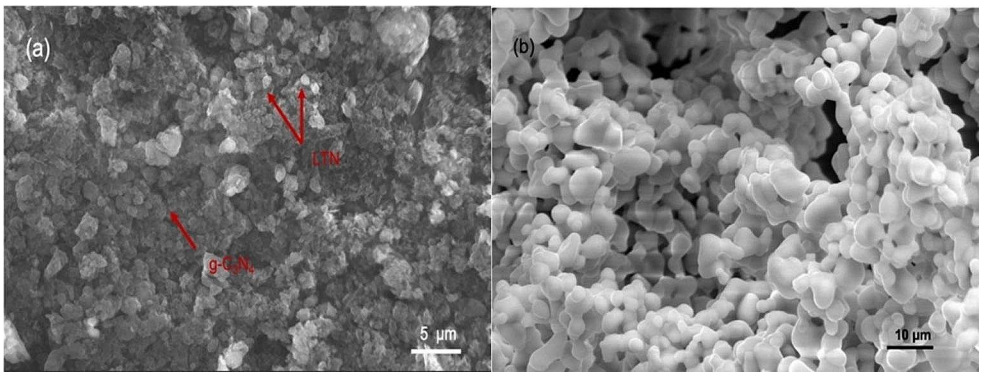

Fig. 4 SEM images of (a) LTN/ g-C_3N_4 heterojunction, and (b) LTN material

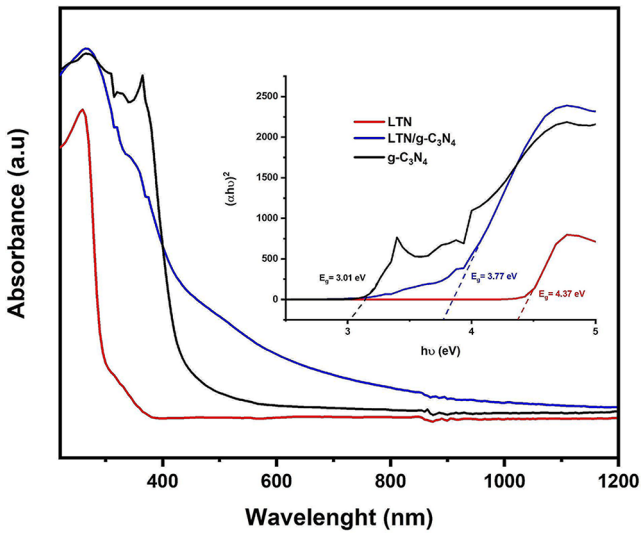

Fig. 5 UV-vis DRS and $(\alpha h\nu)^2$ as a function of photon energy (hν) (insert one)

DRS spectra measurements were used to assess the optical absorption capacity of g-C_3N_4, LTN, and the LTN/g-C_3N_4 heterojunction, as shown in Fig. 5. Two distinct absorption peaks between 300 and 400 nm were observed for g-C_3N_4. Interestingly, the band gap of protonated single-layer g-C_3N_4 was consistent with the LTN/ g-C_3N_4 heterojunction, which showed similar peaks to g-C_3N_4 [35, 36].

To calculate the direct transitions band gaps, the Kubelka-Munk relation (Eq. 4) was employed,

$$\alpha \mathbf{h}\upsilon = \mathbf{A}(\mathbf{h}\upsilon - \mathbf{Eg})^{\mathbf{n}/\mathbf{2}} \tag{4}$$

where α represents the diffuse absorption coefficient, h is the Planck constant, and ν denotes the light frequency.

The plot of $(\alpha h\nu)^2$ vs. hν (shown in the inset of Fig. 5) was used to determine the band gaps. The computed band gaps for g-C_3N_4, LTN/g-C_3N_4, and LTN were found to be 3.01 eV, 3.77 eV, and 4.37 eV, respectively. In contrast to the observed behavior in the LTN sample, it is worth noting that the band gaps of g-C_3N_4 and LTN/g-C_3N_4 exhibited a close correspondence, indicating that they did not simply mix together, but instead formed a heterojunction.

Power density and polarization curves

The evaluation of the Single Chamber Microbial Fuel Cell (MFC) performance was conducted after a duration of 120 h through the utilization of polarization and power density curves. The evaluations were carried out in varying light conditions, including both light and dark conditions, in order to examine the photocatalytic performance of the LTN/ g-C_3N_4-modified carbon cloth electrode. The resistance of the electrode varied from 11 MΩ to 1Ω, and the power output was recorded after the values reached a stable state.

Figure 6(a) illustrates the polarization curves, which indicate a slight increase in the open circuit voltage (OCV) from 703 mV to 710 mV in the presence of light. Theoretically, OCVs in Bio-electrochemical systems (BESs) are closely linked to the concentrations of redox substances [27].

In this particular system, oxygen served as the primary oxidant reduced at the cathode. As the cathode structures were nearly identical and the same gas source (air) was used, the oxygen reduction reaction (ORR) had minimal impact on the change in OCVs [37].

Figure 6(b) displays the power density obtained on the 5th day (after 120 h). It is evident that the maximum power density achieved under light conditions (667.7 mW/m^3) was approximately 65% higher than that observed in the dark conditions (235.64 mW/m^3) for the LTN/ g-C_3N_4-modified electrode. The observed improvement can be attribute to the photocatalytic characteristics of the electrode, enabling the absorption of visible light and promoting the expedited reduction reaction of dissolved O^2 at the cathode through the generation of electron-hole pairs on its surface [38].

The carbon cloth electrode modified with LTN/g-C3N4 demonstrated a significant synergistic effect when exposed to light, leading to a greater power density in comparison to the absence of light. The findings of this study indicatethat LTN/ g-C_3N_4 exhibits promising potential as a highly

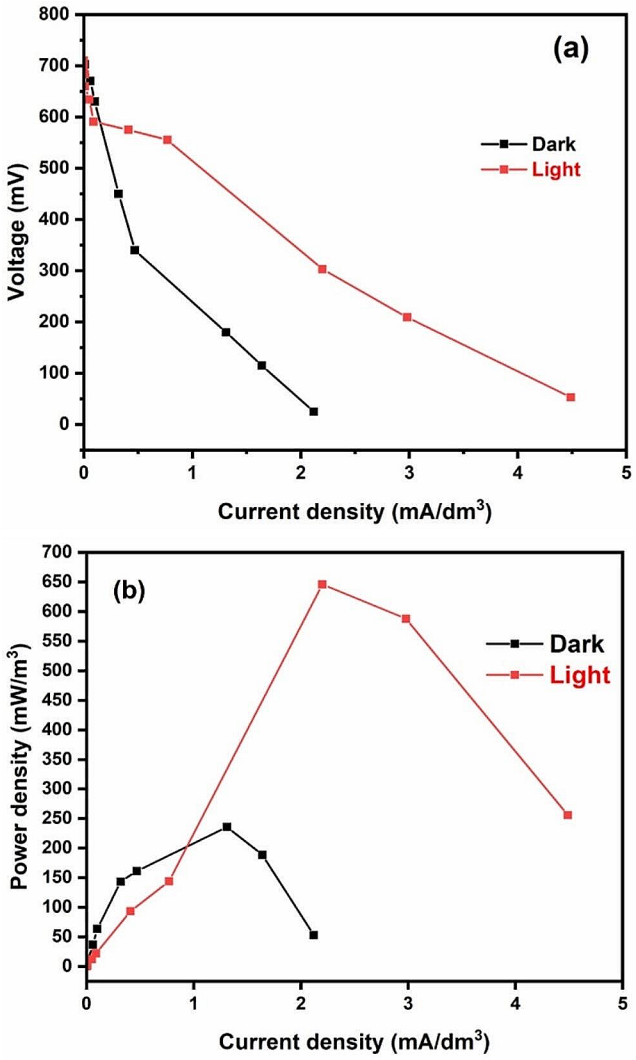

Fig. 6 (**a**) Polarization, and (**b**) Power density curves of LTN/g-C3N4 based MFC

Table 1 Maximum power densities noted in this study with other studies on single chamber MFCs

Cathodes	Power output	Membrane	References
Platinum-coated carbon paper	790 mW/m2		[39]
Non – catalyzed graphite plates	112.2 mW/m2	Nafion 117	[40]
Pt layer coated carbon cloth	0.15 mW/m2)	Nafion	[41]
LiNbO3 coated carbon cloth	131 mW/m3	Nafion (NRE-212)	[11]
LTN/g-C3N4 coated carbon cloth	667.7 mW/m3	Nafion (NRE-212)	This study

effective cathode catalyst, offering a viable alternative to conventional and expensive catalysts such as platinum. This is primarily attributed to its notable catalytic performance and cost-effectiveness.

Comparing the maximum power densities noted in this study with other studies on single chamber MFCs (Table 1), it is clear that significant variations exist. For example, Touach et al. achieved a maximum power density of 40 mW/m^3 using industrial wastewater, which increased to 131 mW/m^3 under UV-visible irradiation [11]. In another study, Cu_2O/rGO cathode catalysts were analyzed alongside commercial Pt/C, and it was observed that the microbial fuel cell (MFC) utilizing Cu_2O/rGO exhibited a greater output voltage (0.223 V) in contrast to the MFC employing commercial Pt/C (0.206 V) [42].

Wastewater treatment

The objective of this study is to investigate the process of bio-photocatalytic oxidation of organic compounds in MFC during electricity generation. Our study was centered on the elimination of COD from a sample of industrial wastewater, which initially had a COD concentration of 1740 mg/L. Figure 7 illustrates the variations in chemical oxygen demand (COD) removal over the course of 24, 48, 72, 96, and 120 h under both illuminated and non-illuminated conditions. The concentration curves illustrated in Fig. 7(a) displayed apparent differences. Under lighted conditions, the removal of COD exhibited a more pronounced and rapid decline, decreasing from an initial concentration of 1740 mg/L to a final concentration of 202 mg/L. This outcome suggests a superior performance in comparison to the COD removal trend observed in the absence of light, where the COD concentration decreased to 583 mg/L.On the initial day of operation, after a duration of 24 h, a modest COD removal value of 19.37% was observed when exposed to the light source depicted in Fig. 7(b). Nevertheless, there was a notable surge in the percentage, rising to 49.6% after a span of 48 h, which was then succeeded by a substantial elevation to 62.42% at the 72-hours, all while the light illumination was sustained. The removal of COD exhibited a continuous improvement, with a value of 75.98% observed at the 96-hous. Subsequently, the removal efficiency reached its maximum value of 88.4% upon completion of the operation, which occurred at the 120-hours. The observed peak removal rate aligns with the peak power generation, suggesting a significant correlation between the removal of COD and the production of electricity. On the other hand, the rate of COD removal in the absence of light conditions reached its maximum value of 66.5%.Furthermore, higher initial concentrations of COD were found to enhance the anaerobic conditions at the anode, leading to a prolonged period of power generation. The enhancement of anaerobic conditions additionally facilitated the removal of COD [43].

In summary, the research findings indicate that bio-electrocatalytic oxidation in a MFC is a viable method for the

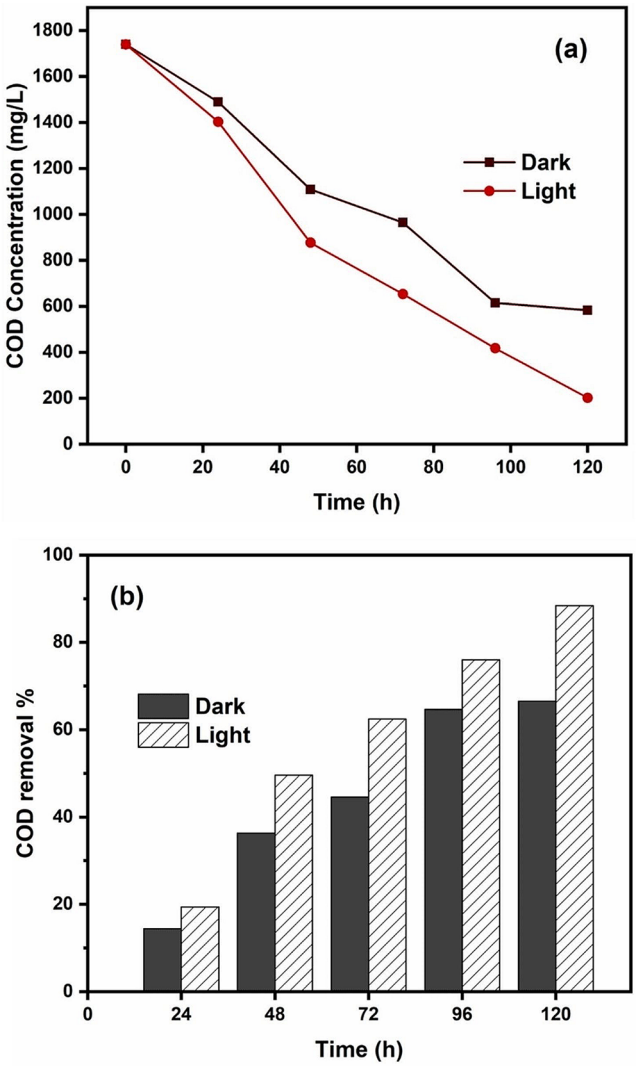

Fig. 7 (**a**) COD concentration, and (**b**) removal percentage noted during MFC treating wastewater

removal of organic compounds. This is supported by the substantial reduction in COD observed under lighted conditions, as compared to the absence of light. The inclusion of light was an essential contributor in enhancing the overall efficacy of the system, resulting in higher levels of COD removal and enhanced power generation. Furthermore, it was observed that higher initial concentrations of COD had a positive influence on the anaerobic conditions, resulting in extended power generation and enhanced removal of COD.

Conclusion

The objective of this study was to evaluate the environmental impacts and energy efficiency of a newly developed composite material incorporated into a carbon cloth cathode, employed for the purpose of converting wastewater into usable energy. To accomplish this goal, a single-chamber MFC was utilized, with the LTN/g-C_3N_4 catalyst employed as a photocatalyst in the cathode, operating under both illuminated and non-illuminated conditions.

The results indicated that the electrode that was developed demonstrated a greater power density when exposed to light (667.7 mW/m^3) compared to when it was in a dark environment (235.64 mW/m^3). Furthermore, the maximum efficiency of COD removal was observed to be 88.4% within a duration of five days in the presence of a light source. The observed outcomes indicate that the LTN/g-C_3N_4 catalyst exhibits favorable characteristics, rendering it a potentially advantageous and economically viable substance for the conversion of organic substances into electrical energy, alongside the concurrent purification of water.

Acknowledgements The authors gratefully acknowledge the support for this project from the national center for scientific and technical research.

Funding This article is based upon work from COST Action [Protection, Resilience, Rehabilitation of damaged environment (PHOENIX), CA19123], supported by COST (European Cooperation in Science and Technology; www.cost.eu).

Data availability Data will be made available on request.

Declarations

Competing interest The authors declare that they have no known competing financial interests or personal relationships that could have appeared to influence the reported in this paper.

References

1. Mazkad, D., Lazar, N. E., Benzaouak, A., Moussadik, A., Hitar, M. E. H., Touach, N., El Mahi, M.: Photocatalytic properties insight of Sm-doped $LiNbO_3$ in ferroelectric Li1− xNb$Sm_{1/3}xO_3$ system. J. Environ. Chem. Eng. **11**(3), 109732 (2023). https://doi.org/10.1016/j.jece.2023.109732
2. Li, H., Jin, C., Mundree, S.: Hybrid environmental and economic assessment of four approaches recovering energy from sludge with variant organic contents. J. Clean. Prod. **153**, 131–138 (Jun. 2017). https://doi.org/10.1016/j.jclepro.2017.03.167

3. Sözen, S., Karaca, C., Alli, B., Orhon, D.: Sludge footprints of municipal treatment plant for the management of net useful energy generation beyond energy neutrality. J. Clean. Prod. **215**, 1503–1515 (Apr. 2019). https://doi.org/10.1016/j.jclepro.2019.01.080
4. Pardee, K., et al.: Portable, On-Demand Biomolecular Manufacturing, *Cell*, vol. 167, no. 1, pp. 248–259.e12, Sep. (2016). https://doi.org/10.1016/j.cell.2016.09.013
5. Zhao, C.E., Gai, P., Song, R., Chen, Y., Zhang, J., Zhu, J.J.: Nanostructured material-based biofuel cells: Recent advances and future prospects. Chem. Soc. Rev. **46**(07), 1545–1564 (2017). 5. Royal Society of Chemistry10.1039/c6cs00044d
6. Liu, H., Ramnarayanan, R., Logan, B.E.: Production of Electricity during Wastewater Treatment Using a Single Chamber Microbial Fuel Cell, Environ Sci Technol, vol. 38, no. 7, pp. 2281–2285, Apr. (2004). https://doi.org/10.1021/es034923g
7. Chaudhuri, S.K., Lovley, D.R.: Electricity generation by direct oxidation of glucose in mediatorless microbial fuel cells, Nat Biotechnol, vol. 21, no. 10, pp. 1229–1232, Oct. (2003). https://doi.org/10.1038/nbt867
8. Xie, J., Hao +, C.-E., Lin, Z.-Q., Gu, P.-Y., Zhang, A.: Nanostructured Conjugated polymers for Energy-Related Applications beyond Solar cells, (2016). [Online]. Available: www.chemasianj.org
9. Bin Song, R., et al.: Aug., Living and Conducting: Coating Individual Bacterial Cells with In Situ Formed Polypyrrole, Angewandte Chemie - International Edition, vol. 56, no. 35, pp. 10516–10520, (2017). https://doi.org/10.1002/anie.201704729
10. Jung, S., Regan, J.M.: Comparison of anode bacterial communities and performance in microbial fuel cells with different electron donors, Appl Microbiol Biotechnol, vol. 77, no. 2, pp. 393–402, Nov. (2007). https://doi.org/10.1007/s00253-007-1162-y
11. Touach, N., et al.: Oct., On the use of ferroelectric material LiNbO3 as novel photocatalyst in wastewater-fed microbial fuel cells, Particuology, vol. 34, pp. 147–155, (2017). https://doi.org/10.1016/j.partic.2017.02.006
12. Zhou, M., Chi, M., Luo, J., He, H., Jin, T.: An overview of electrode materials in microbial fuel cells. J. Power Sources. **196**, 4427–4435 (2011). https://doi.org/10.1016/j.jpowsour.2011.01.012
13. Rojas-Flores, S., et al.: Using lime (Citrus × aurantiifolia), orange (citrus × sinensis), and tangerine (citrus reticulata) waste as a substrate for generating bioelectricity. Environ. Res. Eng. Manage. **76**(3), 24–34 (2020). https://doi.org/10.5755/j01.erem.76.3.24785
14. Feng, Y., et al.: Effects of sulfide on microbial fuel cells with platinum and nitrogen-doped carbon powder cathodes. Biosens. Bioelectron. **35**(1), 413–415 (May 2012). https://doi.org/10.1016/j.bios.2011.08.030
15. Martin, E., Tartakovsky, B., Savadogo, O.: Cathode materials evaluation in microbial fuel cells: A comparison of carbon, Mn2O3, Fe2O3 and platinum materials, Electrochim Acta, vol. 58, no. 1, pp. 58–66, Dec. (2011). https://doi.org/10.1016/j.electacta.2011.08.078
16. Santoro, C., et al.: Iron based catalysts from novel low-cost organic precursors for enhanced oxygen reduction reaction in neutral media microbial fuel cells. Energy Environ. Sci. **9**(7), 2346–2353 (Jul. 2016). https://doi.org/10.1039/c6ee01145d
17. Santoro, C., Serov, A., Artyushkova, K., Atanassov, P.: Platinum group metal-free oxygen reduction electrocatalysts used in neutral electrolytes for bioelectrochemical reactor applications, Current Opinion in Electrochemistry, vol. 23. Elsevier B.V., pp. 106–113, Oct. 01, (2020). https://doi.org/10.1016/j.coelec.2020.06.003
18. Chen, S., et al.: Apr., Electrospun and solution blown three-dimensional carbon fiber nonwovens for application as electrodes in microbial fuel cells, Energy Environ Sci, vol. 4, no. 4, pp. 1417–1421, (2011). https://doi.org/10.1039/c0ee00446d
19. Cai, T., Huang, Y., Huang, M., Xi, Y., Pang, D., Zhang, W.: Enhancing oxygen reduction reaction of supercapacitor microbial fuel cells with electrospun carbon nanofibers composite cathode. Chem. Eng. J. **371**, 544–553 (Sep. 2019). https://doi.org/10.1016/j.cej.2019.04.025
20. Benzaouak, A., et al.: Sep., Ferroelectric LiTaO3 as novel photo-electrocatalyst in microbial fuel cells, Environ Prog Sustain Energy, vol. 36, no. 5, pp. 1568–1574, (2017). https://doi.org/10.1002/ep.12609
21. Louki, S., et al.: Aug., Preparation of new ferroelectric Li0.95Ta0.57Nb0.38Cu0.15O3 materials as photocatalysts in microbial fuel cells, Canadian Journal of Chemical Engineering, vol. 96, no. 8, pp. 1656–1662, (2018). https://doi.org/10.1002/cjce.23117
22. Qi, X., Ren, Y., Liang, P., Wang, X.: New insights in photosynthetic microbial fuel cell using anoxygenic phototrophic bacteria, Bioresource Technology, vol. 258. Elsevier Ltd, pp. 310–317, Jun. 01, (2018). https://doi.org/10.1016/j.biortech.2018.03.058
23. Shi, A., Li, H., Yin, S., Zhang, J., Wang, Y.: H2 Evolution over g-C3N4/CsxWO3 under NIR light. Appl. Catal. B. **228**, 75–86 (Jul. 2018). https://doi.org/10.1016/j.apcatb.2018.01.070
24. Zhang, Y., Zhou, J., Feng, Q., Chen, X., Hu, Z.: Visible light photocatalytic degradation of MB using UiO-66/g-C3N4 heterojunction nanocatalyst, Chemosphere, vol. 212, pp. 523–532, Dec. (2018). https://doi.org/10.1016/j.chemosphere.2018.08.117
25. Hernández-Fernández, F.J., De Los, A.P., Ríos, F., Mateo-Ramírez, M.D., Juarez, L.J., Lozano-Blanco, Godínez, C.: New application of polymer inclusion membrane based on ionic liquids as proton exchange membrane in microbial fuel cell. Sep. Purif. Technol. **160**, 51–58 (Feb. 2016). https://doi.org/10.1016/j.seppur.2015.12.047
26. Larrosa-Guerrero, A., Scott, K., Head, I.M., Mateo, F., Ginesta, A., Godinez, C.: Effect of temperature on the performance of microbial fuel cells, Fuel, vol. 89, no. 12, pp. 3985–3994, Dec. (2010). https://doi.org/10.1016/j.fuel.2010.06.025
27. Logan, B.E., et al.: Microbial fuel cells: Methodology and technology, Environmental Science and Technology, vol. 40, no. 17. pp. 5181–5192, Sep. 01, (2006). https://doi.org/10.1021/es0605016
28. Wang, X., WSPC-MATERIALS FOR SUSTAINABLE ENERGY-Reprint Volume: Book-trim Size:-11in x 8.5in a metal-free polymeric photocatalyst for hydrogen production from water under visible light, (2010). [Online]. Available: www.nature.com/naturematerials
29. Lazar, N., Mazkad, D., Moussadik, A. et al.: High-performance ferroelectric photocatalysts for rapid dye degradation: ZrO_2-doped $LiTa_{0.5}Nb_{0.5}O_3$ under solar UV light. J. Sol-Gel Sci. Technol. **110**, 233–245 (2024). https://doi.org/10.1007/s10971-024-06330-y
30. Mayuri, P., Senthil Kumar, A.: In situ derivatization of an intrinsic iron impurity as a surface-confined iron(II)tris(2,2′-bipyridine) complex on MWCNT and its application to selective electrochemical sensing of DNAs purine bases, Langmuir, vol. 31, no. 21, pp. 5945–5951, Jun. (2015). https://doi.org/10.1021/acs.langmuir.5b00491
31. Guo, J., Li, P., Yang, Z.: A novel Z-scheme g- C3N4/LaCoO3 heterojunction with enhanced photocatalytic activity in degradation of tetracycline hydrochloride, Catal Commun, vol. 122, pp. 63–67, Mar. (2019). https://doi.org/10.1016/j.catcom.2019.01.022
32. Xu, J., Li, Y., Peng, S., Lu, G., Li, S.: Eosin Y-sensitized graphitic carbon nitride fabricated by heating urea for visible light photocatalytic hydrogen evolution: The effect of the pyrolysis temperature of urea. Phys. Chem. Chem. Phys. **15**(20), 7657–7665 (May 2013). https://doi.org/10.1039/c3cp44687e
33. Vilarinho, P.M., Barroca, N., Zlotnik, S., Félix, P., Fernandes, M.H.: Are lithium niobate ($LiNbO_3$) and lithium tantalate ($LiTaO_3$) ferroelectrics bioactive? Mater. Sci. Eng. C Mater.

Biol. Appl. **39**(1), 395–402 (2014). https://doi.org/10.1016/j.msec.2014.03.026
34. Ono, H., Koyanagi, K.I.: Infrared absorption peak due to Ta = O bonds in Ta_2O_5 thin films. Appl. Phys. Lett. **77**(10), 1431–1433 (2000). https://doi.org/10.1063/1.1290494
35. Zhang, X., Xie, X., Wang, H., Zhang, J., Pan, B., Xie, Y.: Enhanced photoresponsive ultrathin graphitic-phase C3N 4 nanosheets for bioimaging, J Am Chem Soc, vol. 135, no. 1, pp. 18–21, Jan. (2013). https://doi.org/10.1021/ja308249k
36. Zhang, X., et al.: Jul., Single-layered graphitic-C3N4 quantum dots for two-photon fluorescence imaging of cellular nucleus, Advanced Materials, vol. 26, no. 26, pp. 4438–4443, (2014). https://doi.org/10.1002/adma.201400111
37. Chen, J., Lv, Y., Wang, Y., Ren, Y., Li, X., Wang, X.: Endogenous inorganic carbon buffers accumulation and self-buffering capacity enhancement of air-cathode microbial fuel cells through anolyte recycling. Sci. Total Environ. **676**, 11–17 (Aug. 2019). https://doi.org/10.1016/j.scitotenv.2019.04.282
38. Wang, S., Yang, X., Zhu, Y., Su, Y., Li, C.: Solar-assisted dual chamber microbial fuel cell with a CuInS2 photocathode. RSC Adv. **4**(45), 23790–23796 (2014). https://doi.org/10.1039/c4ra02488e
39. Cho, Y.K., Donohue, T.J., Tejedor, I., Anderson, M.A., McMahon, K.D., Noguera, D.R.: Development of a solar-powered microbial fuel cell. J. Appl. Microbiol. **104**(3), 640–650 (2008). https://doi.org/10.1111/j.1365-2672.2007.03580.x
40. Chandra, R., Modestra, J.A., Venkata Mohan, S.: Biophotovoltaic cell to harness bioelectricity from acidogenic wastewater associated with Microbial Community Profiling, Fuel, vol. 160, pp. 502–512, Nov. (2015). https://doi.org/10.1016/j.fuel.2015.07.090
41. Lai, Y.C., Liang, C.M., Hsu, S.C., Hsieh, P.H., Hung, C.H.: Polyphosphate metabolism by purple non-sulfur bacteria and its possible application on photo-microbial fuel cell, J Biosci Bioeng, vol. 123, no. 6, pp. 722–730, Jun. (2017). https://doi.org/10.1016/j.jbiosc.2017.01.012
42. Xin, S., et al.: Electricity generation and microbial community of single-chamber microbial fuel cells in response to Cu2O nanoparticles/reduced graphene oxide as cathode catalyst. Chem. Eng. J. **380** (Jan. 2020). https://doi.org/10.1016/j.cej.2019.122446
43. Zhang, L., Fu, G., Zhang, Z.: High-efficiency salt, sulfate and nitrogen removal and microbial community in biocathode microbial desalination cell for mustard tuber wastewater treatment. Bioresour Technol. **289** (Oct. 2019). https://doi.org/10.1016/j.biortech.2019.121630